Tetranuclear Complexes Containing Bimetallic Tetracarboxylates and Ferrocene − Models for Subunits of One-Dimensional Organometallic Polymers

Wen-Mei Xue[a] and Fritz E. Kühn*[a]

Keywords: Metal-metal interactions / Molybdenum / Polymers / Rhodium / Ferrocene

The tetranuclear compounds $M_2(O_2C\text{-}R)_4L_2$ [M = Rh, R = nC_7H_{15}, L = ferrocenyl-4-pyridylacetylene (FPA) (**1a**); M = Rh, R = CH_3, L = FPA (**1b**); M = Mo, R = CF_3, L = FPA (**2b**); M = Rh, R = nC_7H_{15}, L = 4-ferrocenylpyridine (FP) (**3a**); M = Rh, R = CH_3, L = FP (**3b**); M = Mo, R = nC_7H_{15}, L = FP (**4a**); M = Mo, R = CF_3, L = FP (**4b**)] have been synthesized by the reaction of bimetallic tetracarboxylates with L in a 1:2 ratio, in a noncoordinating solvent. The reaction of $Mo_2(O_2C\text{-}nC_7H_{15})_4$ with FPA in a 1:2 molar ratio leads to a trinuclear compound $Mo_2(O_2C\text{-}nC_7H_{15})_4$(FPA) (**2a**). A soluble oligomer $[Rh_2(O_2C\text{-}nC_7H_{15})_4(BPEF)]_n$ [**5**, BPEF = 1,1′-bis(4-pyridylethynyl)ferrocene] is obtained by the reaction of $Rh_2(O_2C\text{-}nC_7H_{15})_4$ with BPEF in a 1:1 ratio in CH_2Cl_2 or $CHCl_3$, whereas the reaction of $Mo_2(O_2C\text{-}nC_7H_{15})_4$ with BPEF leads to a pentanuclear compound $[Mo_2(O_2C\text{-}nC_7H_{15})_4]_2$(BPEF) (**6**), even when BPEF is in excess. ^{1}H NMR, Raman, UV/Vis absorption spectroscopy and cyclic voltammetry indicate that the metal-metal bonds are weakened by the metal-axial ligand interaction and the donor-acceptor interactions occurring between the building blocks of the multinuclear compounds and oligomers. The interaction between the bimetallic centers and the ferrocene moiety is enhanced by shortening the distances between them. This shortening is achieved by modification of the axial ligand from FPA to FP. A significant electronic communication between the ferrocene units is not observed.

Introduction

Since Cotton's recognition of metal-metal bonds in 1964, the field of multiple bonds between metal atoms has been an active area of research in modern coordination chemistry. Oligomers and polymers containing metal-metal bonds in the backbone may display novel optical and magnetic properties.[1] Two general types of one-dimensional polymers can be envisaged, and these are shown in Scheme 1.[2a]

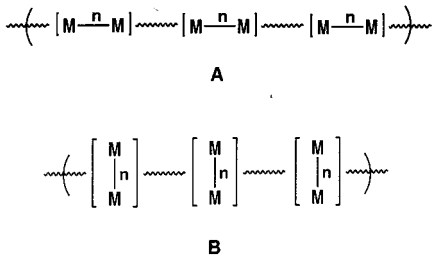

Scheme 1

In **A**, the M−M axis associated with the M−M bond is parallel to the propagating axis, whereas in **B** the M−M axis is perpendicular. Examples of the latter type are oligomers composed of $Mo_2(O_2C\text{-}tBu)_2$ and $^-OOC-R-COO^-$ units, which have been reported by Chisholm et al.[2] Polymers of type **A** can be constructed by axial coordination of the linking ligands to the bimetallic complexes. A number of bimetallic tetracarboxylates have been linked by bidentate organic axial ligands, resulting in polymeric species.[3] These types of polymers have the advantage of being readily accessible. A wide diversity of bimetallic centers, equatorial ligands and axial linkages can be used. As a result the polymer properties, such as solubility, strength of metal-axial ligand interaction, electronic and electrochemical behaviors, can be easily tuned. However, to the best of our knowledge, examples of these types of oligomers and polymers with organometallic spacing groups are very rare.[4] Nevertheless, organometallic linkers are interesting alternatives to organic linkers. Several of these organometallic complexes can be quite easily obtained and can be modified to a significant degree by well-established synthetic strategies. A much broader variety of potential product molecules are available than with simple organic molecules.

We attempted to incorporate bimetallic units into one-dimensional organometallic polymers of type **A**.[4] As this area of chemistry is relatively new, we chose to work with dimolybdenum(II) and dirhodium(II) tetracarboxylates since their molecular and electronic structures have been extensively studied.[1] Conjugated ligands containing a ferrocene moiety were selected as bridging ligands, due to the favorable electrochemical properties of ferrocene, and the comparatively easy accessibility and high synthetic yields of these complexes.

We recently reported oligomers with backbones containing 1,1′-bis(4-pyridylethynyl)ferrocene (BPEF) and bimetallic tetracarboxylates. However, it was found that these oligomers are insoluble in noncoordinating solvents, and the use of strongly coordinating solvents, such as CH_3CN

[a] Anorganisch-Chemisches Institut der Technischen Universität München,
Lichtenbergstraße 4, 85747 Garching bei München, Germany
Fax: (internat.) +49−(0)89/289-13473
E-mail: fritz.kuehn@ch.tum.de

  1434−1948/01/0808−2041 $ 17.50+.50/0

and THF, resulted in the destruction of the polymer chain due to replacement of the comparatively weakly coordinating BPEF ligands by solvent molecules.[4a] The poor solubility hinders complete characterization and detailed examination of their properties. An important step forward is to make the oligomers and polymers soluble in both coordinating and noncoordinating solvents. In this work we report on how this can be achieved. Furthermore, the axial ligands for the model compounds are modified from ferrocenyl-4-pyridylacetylene (FPA) to 4-ferrocenylpyridine (FP), in order to investigate the effect on the electronic coupling between the two ferrocene units resulting from the decreased distance between them.

Results and Discussion

Preparation and Characterization

The reactions of the bimetallic tetracarboxylates with the monodentate ligands FPA or FP, in a 1:2 molar ratio, led to the formation of the tetranuclear complexes **1a**, **1b**, **2b**, **3a, 3b**, **4a** and **4b** (Scheme 2). Compound **2a** has only one axial ligand due to the relatively weak metal-axial ligand interaction between $Mo_2(O_2C\text{-}nC_7H_{15})_4$ and FPA. Similarly, the reaction of $Mo_2(O_2C\text{-}nC_7H_{15})_4$ with a bidentate ligand BPEF in a 1:1 molar ratio gave a pentanuclear complex **6**, whereas BPEF with $Rh_2(O_2C\text{-}nC_7H_{15})_4$ formed the oligomeric compound **5**.

While the dirhodium complexes **1a**, **1b**, **3a**, **3b**, and **5** are air-stable, the dimolybdenum complexes **2a**, **2b**, **4a**, **4b**, and **6** decomposed when exposed to air for a few hours in the solid state, and within a couple of minutes in solution. The bimetallic compounds containing long-chain carboxylates are very soluble. The oligomer **5** is soluble in some noncoordinating solvents such as CH_2Cl_2 and $CHCl_3$, in contrast to the previously reported oligomers $[Rh_2(O_2CCH_3)_4(BPEF)]_n$, $[Rh_2(O_2CCF_3)_4(BPEF)]_n$, and $[Mo_2(O_2CCF_3)_4(BPEF)]_n$ which are insoluble in any noncoordinating solvent and decompose in coordinating solvents.[4]

The complexes were characterized by elemental analysis, NMR, solid state IR and Raman spectroscopies. Selected spectroscopic data are listed in Table 1.

The resonance signals for the pyridyl protons of the dirhodium complexes **1a**, **1b**, **3a**, **3b** and **5** appear at a lower field than those of the respective free ligands FPA, FP and BPEF. In contrast, upfield shifts of the pyridyl protons are observed in the dimolybdenum complexes. The coordination of the pyridyl ligands used here to form complexes with $Rh_2(O_2CCH_3)_4$ and $Rh_2(O_2C\text{-}nC_7H_{15})_4$, leads to a comparable downfield shift of the α-pyridyl protons ($\Delta^1H \approx 0.6-0.8$ ppm), reflecting the tendency of dirhodium(II) centers to bind axial ligands. The chemical shifts of the α-pyridyl protons of **2b** ($\delta = 8.03$) and **4b** ($\delta = 7.90$) differ significantly from those of the respective free ligands FPA ($\delta = 8.53$) and FP ($\delta = 8.45$), as a result of the relatively strong Lewis acidity of $Mo_2(O_2CCF_3)_4$. However, those of **2a** ($\delta = 8.30$) and **4a** ($\delta = 8.21$) differ from the free ligands by only

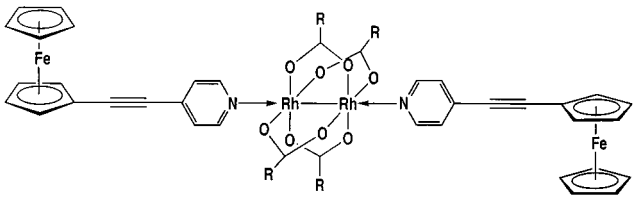

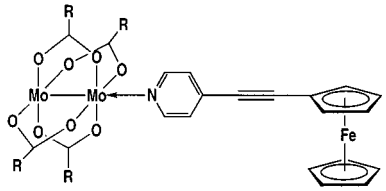

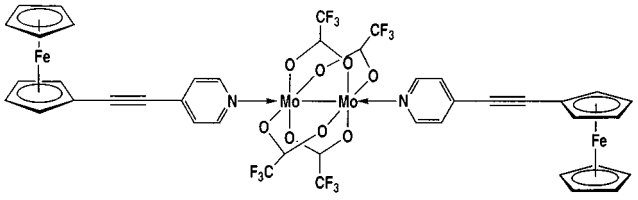

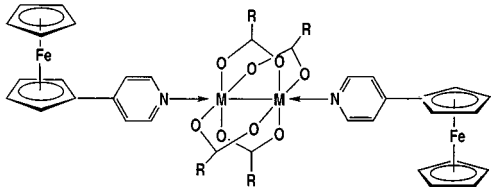

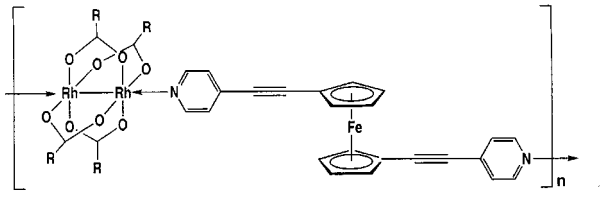

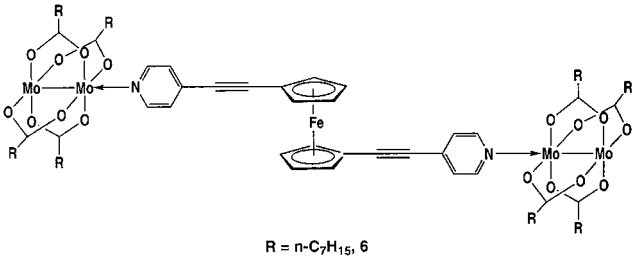

Scheme 2

Table 1. Selected characterization data of the compounds and their precursors

Compound[a]	δ(^{1}H)C_5H_4N(α)	δ(^{1}H)C_5H_4N(β)	δ(^{1}H)C_5H_4(α)	δ(^{1}H)C_5H_4(β)	δ(^{1}H)C_5H_5	δ(^{1}H)CH_2(2)	δ(^{1}H)CH_2(3)	ν(C≡C) cm^{-1}	ν(M−M) cm^{-1}
1a	9.24 s, br.	7.69 s, br.	4.60 s	4.33 s	4.29 s	2.10 t	1.42 m	2207	339
1b	9.11 s, br.	7.72 d	4.63 t	4.38 t	4.31 s	−	−	2205	341
2a	8.30 s, br.	7.22 s, br.	4.50 s	4.28 s	4.22 s	2.92t	1.85 m	2202	397
2b	8.03 d	7.24 d	4.53 t	4.33 t	4.23 s	−	−	2207	362
FPA	8.53 d	7.32 d	4.54 t	4.31 t	4.25 s	−	−	2210	−
3a	9.13 d	7.67 d	4.86 t	4.50 t	4.14 s	2.12 t	1.45 m	−	324
3b	9.21 d	7.70 d	4.87 t	4.51 t	4.14 s	−	−	−	320
4a	8.21 d	7.21 d	4.66 t	4.40 t	4.00 s	2.96 t	1.87 m	−	400
4b	7.90 d	7.19 d	4.64 t	4.42 t	3.99 s	−	−	−	360
FP	8.45 d	7.30 d	4.71 t	4.41 t	4.03 s	−	−	−	−
5	9.26 d	7.72 d	4.71 s	4.50 s	−	2.11 t	1.43 m	2211	342
6	8.31 d	7.15 d	4.54 t	4.35 t	−	2.90 t	1.83 m	2207	397
BPEF	8.46 d	7.19 d	4.57 t	4.37 t	−	−	−	2208	−
$Rh_2(O_2C$-$nC_7H_{15})_4$	−	−	−	−	−	2.34 t	1.54 m	−	344
$Mo_2(O_2C$-$nC_7H_{15})_4$	−	−	−	−	−	2.82 t	1.80 m	−	401

ca. δ = 0.23, reflecting a rather weak metal-axial ligand interaction in the $Mo_2(O_2C$-$nC_7H_{15})_4$ derivatives. The ^{1}H NMR signal of the CH_3CO_2 group is shifted downfield from δ = 1.76 in the axial-ligand free $Rh_2(O_2CCH_3)_4$, to δ = 1.88 in the FPA-coordinated complex **1b** and to δ = 1.93 in the FP ligated complex **3b**. This demonstrates that electron density must be donated back to the axial ligands. In the cases of the tetraoctanoate bimetallic derivatives, the chemical shifts of only the CH_2(2) and CH_2(3) protons are affected by the coordination of axial ligands. The resonances of the CH_2(2) moiety are shifted upfield from δ = 2.34 in the axial-ligand free $Rh_2(O_2C$-$nC_7H_{15})_4$ to ca. δ = 2.11 in the complexes **1a**, **3a** and **5**. The signals of CH_2(3) are shifted from δ = 1.54 to ca. δ = 1.43. The resonances of CH_2(2) and CH_2(3) in the cases of the dimolybdenum complexes **2a**, **4a** and **6**, are shifted downfield from δ = 2.82 [$Mo_2(O_2C$-$nC_7H_{15})_4$] to δ = 2.90−2.96 [CH_2(2)] and from δ = 1.80 to δ = 1.83−1.87 [CH_2(3)]. The ferrocene proton resonances in the FPA-coordinated complexes do not show a significant difference relative to those of the free ligand (Table 1). However, the ferrocene protons of the FP derivatives, especially the dirhodium complexes, differ notably in their chemical shifts from the free ligand as a result of the shortened distance between the ferrocene moiety and the M_2 center, thus enhancing their electronic interaction. It is also interesting to note that the ferrocene proton resonances of oligomer **5** [$\delta(H_\alpha)$ = 4.71, $\delta(H_\beta)$ = 4.50] are shifted downfield from those of the free ligand BPEF [$\delta(H_\alpha)$ = 4.57, $\delta(H_\beta)$ = 4.37], whereas the signals of its tetranuclear model complex **1a** [$\delta(H_\alpha)$ = 4.60, $\delta(H_\beta)$ = 4.33] are quite similar to the free ligand FPA [$\delta(H_\alpha)$ = 4.54, $\delta(H_\beta)$ = 4.31]. This might indicate a better electronic delocalization in the oligomer than in the tetranuclear model compound.

As demonstrated previously, Raman spectroscopy is more informative than single-crystal X-ray analysis with regard to metal-metal interactions.[5] The strong Raman band centered at 324 cm^{-1} for complex **3a** is unambiguously assigned to the stretching frequency of the Rh−Rh bond, which is shifted 20 cm^{-1} lower in energy relative to the axial-ligand free complex $Rh_2(O_2C$-$nC_7H_{15})_4$ [ν(Rh−Rh) = 344 cm^{-1}]. This observation is probably due to the fact that coupling between the Rh−Rh stretching mode and the Rh-axial ligand stretching mode leads to a weakening of the Rh−Rh interaction. However, the coupling between the dirhodium center and the axial ligands in the cases of the FPA and BPEF derivatives is weaker than in the FP-coordinated compound **3a**, as indicated by the fact that the Rh−Rh vibration frequencies of compounds **1a** (339 cm^{-1}) and **5** (342 cm^{-1}) are very similar to that of the parent precursor. The same behavior has also been observed in the cases of the $Rh_2(O_2CCH_3)_4$ derivatives. The compound $Rh_2(O_2CCH_3)_4(FP)_2$ shows a Rh−Rh vibration at 320 cm^{-1}, which is 31 cm^{-1} lower in energy than the parent compound $Rh_2(O_2CCH_3)_4$ (ν(Rh−Rh) = 351 cm^{-1}). However, compounds **1b** and $[Rh_2(O_2CCH_3)_4(BPEF)]_n$ display their Rh−Rh vibrations at 341 and 343 cm^{-1}, respectively, with a deviation of about 10 cm^{-1} from the vibration of the parent precursor. These observations also demonstrate that $Rh_2(O_2CCH_3)_4$ and $Rh_2(O_2C$-$nC_7H_{15})_4$ have a similar tendency to bind axial ligands, the weakening of the metal-metal bond is mainly dependent on the donor strength of the axial ligands. Since $Mo_2(O_2C$-$nC_7H_{15})_4$ is only weakly bonded to the axial ligands, the Mo-Mo vibrations of complexes **2a**, **4a** and **6** display their bands at 397, 400 and 397 cm^{-1}, respectively, with a deviation within the measurement error range from that of the free precursor (401 cm^{-1}). Due to the relatively strong metal-axial ligand interaction in the cases of the $Mo_2(O_2CCF_3)_4$ derivatives, the Mo−Mo vibration is shifted to lower energies (ca. 27−33 cm^{-1} relative to the precursor).

In order to demonstrate an oligomer chain growth in solution, ^{1}H NMR investigations were performed on a mixture of $Rh_2(O_2C$-$nC_7H_{15})_4$ and BPEF, in different molar ratios in $CDCl_3$. The concentrations of the compounds in solution were in the range of 2×10^{-3} to 4×10^{-3} M. The measurements were performed after the solution was stirred at room temperature for 1 h. The results of this ^{1}H NMR study are summarized in Table 2, the data for oligomer **5**

Table 2. ^{1}H NMR spectroscopic data of mixtures of BPEF (A) and $Rh_2(O_2C\text{-}nC_7H_{15})_4$ (B) in $CDCl_3$ at room temperature

Sub-stance[a]	$C_5H_4N(\alpha)$		$C_5H_4N(\beta)$		$C_5H_4(\alpha)$		$C_5H_4(\beta)$		$CH_2(2)$		$CH_2(3)$		$CH_2(4-7)$		CH_3	
	δ(^{1}H)	I[b]	δ(^{1}H)	I[b]	δ(^{1}H)	I[b]	δ(^{1}H)	I[b]	δ(^{1}H)	I[b]	δ(^{1}H)	I[b]	δ(^{1}H)	I[b]	δ(^{1}H)	I[b]
A_1B_2	9.09 s, br.	3.8 (4)	7.72 d	4.0 (4)	4.71 s	3.9 (4)	4.50 s	4.0 (4)	2.13 t	15 (16)	1.39−1.46 m	18 (16)	1.08−1.26 m	63 (64)	0.84 t	23 (24)
A_2B_3	9.17 s, br.	7.5 (8)	7.73 d	8.0 (8)	4.71 s	7.9 (8)	4.51 s	7.6 (8)	2.13 t	24 (24)	1.39−1.46 m	28 (24)	1.10−1.26 m	102 (96)	0.84 t	38 (36)
A_3B_4	9.23 s	12 (12)	7.73 d	12 (12)	4.72 s	12 (12)	4.50 s	12 (12)	2.12 t	31 (32)	1.39−1.46 m	34 (32)	1.11−1.27 m	130 (128)	0.84 t	48 (48)
A_4B_5	9.23 s	16 (16)	7.71 d	16 (16)	4.71 s	16 (16)	4.50 s	16 (16)	2.11 t	38 (40)	1.39−1.47 m	42 (40)	1.11−1.25 m	152 (160)	0.85 t	54 (60)
A_5B_6	9.26 d	20 (20)	7.73 d	20 (20)	4.72 s	20 (20)	4.50 s	20 (20)	2.12 t	45 (48)	1.39−1.47 m	50 (48)	1.10−1.26 m	195 (192)	0.85 t	72 (72)
5	9.26 d	4 (4)	7.72 d	4 (4)	4.71 s	4 (4)	4.50 s	4 (4)	2.11 t	8.9 (8)	1.39−1.47 m	9.0 (8)	1.10−1.27 m	38 (32)	0.85 t	13 (12)
A	8.46 d	4	7.19 d	4	4.57 t	4	4.37 t	4	−	−	−	−	−	−	−	−
B	−	−	−	−	−	−	−	−	2.34 t	8	1.54 m	8	1.18 m	32	0.82 t	12

[a] A_mB_n represents the molar ratio of BPEF to $Rh_2(O_2C\text{-}nC_7H_{15})_4$ which is *m*:*n*; the concentration of subunit is in the range of 2×10^{-3} to 4×10^{-3} M. − [b] I = integration, the calculated data are in parenthesis.

and the precursors $Rh_2(O_2C\text{-}nC_7H_{15})_4$ and BPEF are also included for comparative purposes. It is interesting to note that the species present in solution depends on the molar ratio of the two precursor complexes. The oligomer chain grows as the molar ratio of BPEF:$Rh_2(O_2C\text{-}nC_7H_{15})_4$ (A:B) increases. The spectrum of the solution containing BPEF and $Rh_2(O_2C\text{-}nC_7H_{15})_4$ in a 5:6 ratio is quite similar to that of the isolated oligomer **5**. This observation suggests that the repeating unit of oligmer **5** is at least 5, and its molecular weight is not lower than 5832 amu.

Electronic Absorption Spectra

The electronic absorption spectroscopic data of the complexes and their precursors are given in Table 3. Figure 1 presents a comparison of the UV/Vis spectra of oligomer **5** and its precursors. The characteristic absorptions of the product complexes are similar to those of the ferrocenyl pyridine precursors. In general, a peak at ca. 330−370 nm and a broad band centered at ca. 420−480 nm are assigned to d−d transitions in the ferrocene unit.[4,6] The fairly intense bands at λ = 320 nm are assigned to a π→π* pyridyl transition. A comparison of the lowest energy d−d transition band between compounds **1a**, **1b**, **2a**, **2b** and their axial ligand FPA, reveals that the coordination of FPA does not noticeably disturb the d−d transition energy in the ferrocene unit. This is probably due to the relatively weak metal-axial ligand interaction, weak donor ability of FPA and the long distance between the ferrocene moiety and the

Table 3. UV/Vis absorption spectroscopic data and cyclic voltammetric data of the compounds and their precursors

Material	λ_{max}/nm (ε/M^{-1} cm^{-1})[a]	$E(\Delta E_p)$, $Fe^{3+/2+}$/V[a][b]	$E(\Delta E_p)$, $[M_2]^{5+/4+}$/V[a] [b]
1a	268 (32900), 308 (30900), 365 (10700), 450 (2620)	0.18 (75)	0.49 (114)
1b	267 (35200), 308 (32800), 365 (13600), 451 (3040)	0.18 (61)	0.52 (82)
2a	261 (19500), 303 (14700), 450 (1030)	0.23 (80)	0.04 (73)
2b	254 (31800), 305 (37400), 451 (23400)	0.17 (80)	
FPA	252 (13700), 304 (12800), 352 (2320), 449 (760)	0.12 (72)	−
3a	283 (41500), 348 (11500), 456 (br., 2160)	0.15 (83)	0.44 (73)
3b	284 (30000), 341 (9290), 458 (br., 1930)	0.15 (74)	0.48 (69)
4a	289 (26000), 364 (sh, 3900), 476 (br., 2000)	0.28 (85)	0.05 (115)
4b	284 (33900), 330 (sh, 11700), 463 (br., 2250)	0.30 (92)	
FP	279 (12400), 340 (2110), 454 (630)	0.13 (104)	−
5	269 (33500), 317 (24700), 362 (11600), 450 (2130)[d]	0.33 (110)[c]	
6	261 (35300), 300 (26100), 420 (4470)	[e]	
BPEF	261 (26100), 281 (20900), 311 (19600), 350 (sh, 4160), 457 (1040)	0.28 (110)	−
$Rh_2(O_2CCH_3)_4$	434 (170, 551 (230)[f]	−	0.90 (78)
$Rh_2(O_2C\text{-}nC_7H_{15})_4$	253 (9390), 420 (200), 657 (270)	−	0.81 (102)
$Mo_2(O_2C\text{-}nC_7H_{15})_4$	261 (7800), 289 (7570), 420 (280)	−	0.04 (107)

[a] Measured in deoxygenated CH_2Cl_2 solutions except if otherwise stated. − [b] The typical concentration of the complexes is 10^{-3} M. Potentials are vs. the ferrocenium/ferrocene couple (0.00V with ΔE_p = 95 mV); scan rate is 50 mV/s; $\Delta E_p = E_{pa} - E_{pc}$ (mV). − [c] Measured in $CDCl_3$. It is not assigned with surety. − [d] Molarity is based on the repeating unit. − [e] Measurement is not successful. − [f] Measured in CH_3CN.

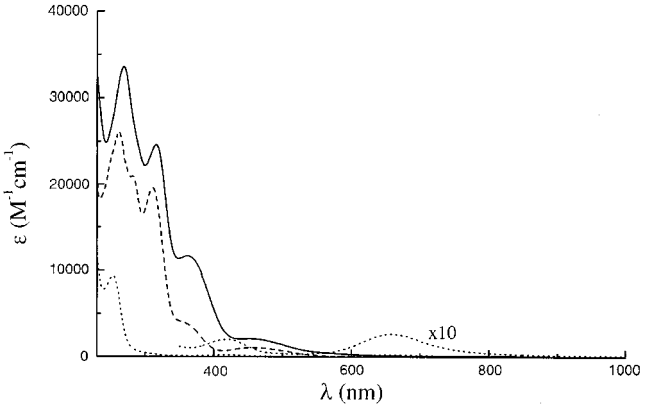

Figure 1. UV/Vis absorption spectra of $[Rh_2(O_2C\text{-}nC_7H_{15})_4\text{-}(BPEF)]_n$ (**5**, solid line), $Rh_2(O_2C\text{-}nC_7H_{15})_4$ (dotted line) and BPEF (dashed line) in CH_2Cl_2 at room temperature

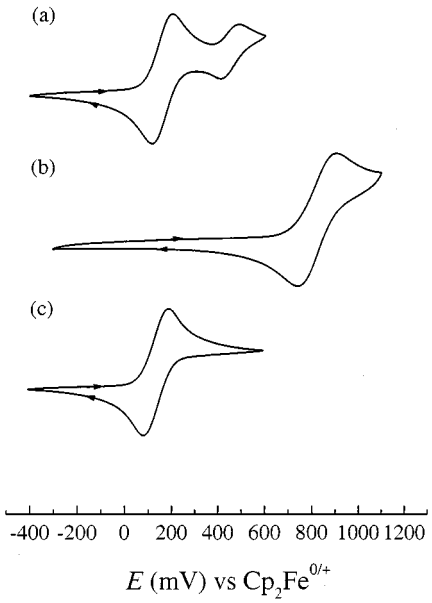

Figure 2. Cyclic voltammograms of (a) $Rh_2(O_2C\text{-}nC_7H_{15})_4(FP)_2$ (**3a**), (b) $Rh_2(O_2C\text{-}nC_7H_{15})_4$ and (c) FP at the same scan rate of 50 mV/s in CH_2Cl_2 with 0.1 M TBAH at room temperature

dimetallic centers. The ^1H NMR spectroscopic data described above are also in good agreement with this observation. However, in the cases of the FP derivatives, the lowest energy d−d transition band is shifted from 454 nm in FP to 456 nm in **3a**, 458 nm in **3b**, 463 nm in **4b** and 476 nm in **4a**. This again demonstrates that the shortening of the distance between the ferrocene unit and the bimetallic centers increases the electronic interaction between the building blocks. Even though the bathochromic shifts of the respective UV/Vis transitions are not quite pronounced, the stronger extinction coefficients of the products vs. their precursors probably indicate a better electronic delocalization. However, a metal-to-metal (ferrocene to dimetallic center) charge transfer (MM′CT) band is not found in the electronic absorption spectra (200−1100 nm).

Electrochemical Properties

As depicted in Figure 2, the cyclic voltammogram of complex **3a** in CH_2Cl_2 exhibits two subsequently reversible anodic couples. The first oxidation with $E_{1/2} = 0.15$ V is assigned to the oxidation of the two ferrocene units, whereas the second with $E_{1/2} = 0.44$ V is due to the oxidation process of the $[Rh_2]^{5+/4+}$ couple. The coordination of dirhodium(II) by FP results in a pronounced cathodic shift of the $[Rh_2]^{5+/4+}$ couple from the parent $Rh_2(O_2C\text{-}nC_7H_{15})_4$ (0.81 V), but a weak anodic shift of the $Fe^{3+/2+}$ couple from the free ligand FP (0.13 V). The same results were obtained when comparing the electrochemical behavior of the product molecules **1a**, **1b** and **3b** with their respective precursors (Table 3). The fact that the oxidation potentials of the $Fe^{3+/2+}$ couple for the above mentioned complexes are close to ones of the free ligands testifies the low electronic perturbation of the ferrocene unit caused by the linkage to the dirhodium centers. However, the $[Rh_2]^{5+/4+}$ oxidation potential is significantly shifted by the electron-donor effect of the pyridyl ligands.

The electrochemical experiments performed with the oligomer **5** were not very successful, only one reversible oxidation couple with $E_{1/2} = 0.33$ V is observed. We are not able to assign this to the oxidation process of the $[Rh_2]^{5+/4+}$ or $Fe^{3+/2+}$ couple without any doubt. Nonetheless, all the tetranuclear model complexes show a single oxidation process for the ferrocene units. We believe that the absence of electronic communication in the tetranuclear model complexes excludes the possibility of electronic communication in the corresponding polymers.

Conclusions

One-dimensional organometallic oligomers with a backbone consisting of bimetallic tetracarboxylates and π-conjugated ferrocene derivatives are generated by mixing the precursor compounds in noncoordinating solvents at room temperature. The solubility of the oligomers in noncoordinating solvents is enhanced by using octanoates as equatorial ligands. These complexes are soluble in both noncoordinating and coordinating solvents, thus enabling a complete characterization and a more detailed examination of their properties than was possible for related complexes previously examined. The electronic and electrochemical investigations of the tetranuclear model compounds indicate that the ferrocene units are electronically noncommunicating, despite the fact that the axial ligands are modified from FPA to FP which remarkably shortens the distance between the two ferrocene units. However, especially in the case of complexes consisting of Rh−Rh units and FP as the axial ligands, the Rh−Rh interaction is significantly influenced (weakened) by the coordinating ligands.

Experimental Section

General: The preparations and manipulations were carried out under an oxygen- and water-free argon atmosphere using the standard

Schlenk techniques. Solvents were dried by standard procedures, distilled, and kept under argon over molecular sieves. The syntheses of the ligands ferrocenyl-4-pyridylacetylene (FPA), 1,1′-bis(4-pyridylethynyl)ferrocene (BPEF), and the tetranuclear complexes $Rh_2(O_2CCH_3)_4(FPA)_2$ (**1b**), $Mo_2(O_2CCF_3)_4(FPA)_2$ (**2b**) have been described previously.[4] 4-Ferrocenylpyridine (FP) was prepared by a literature method.[7]

Elemental analyses were performed in the Mikroanalytisches Labor of the TU München in Garching. − ^1H, ^{13}C and ^{19}F NMR spectra were obtained with Joel JNM GX-400 spectrometers. − IR spectra were recorded on a Perkin−Elmer FT-IR spectrometer using KBr pellets as the IR matrix. − Raman spectra of the solid samples were measured on a Bio-Rad FTS 575C spectrometer using a 1064 μm excitation of the Nd:YAG laser. − Electronic absorption spectra were obtained by using a Perkin−Elmer Lambda 2 UV/Vis spectrometer. − Cyclic voltammograms were recorded with a computer-controlled Model 173 Potentiostat/galvanostat (EG&G Princeton Applied Research) in argon-saturated dried solutions, with tetrabutylammonium hexafluorophosphate (TBAH, 0.1 M) as the supporting electrolyte. The working electrode was platinum and the reference electrode was silver. Potentials are quoted vs. the ferrocene-ferrocenium couple as an internal standard.

$Rh_2(O_2C$-*n*$C_7H_{15})_4$: Prepared by ligand exchange reaction between $Rh_2(O_2CCH_3)_4$ and $CH_3(CH_2)_6COOH$ according to a literature method.[8] − $C_{32}H_{60}O_8Rh_2$ (778.24): calcd. C 49.34, H 7.77; found C 48.74, H 7.80. − IR (KBr): $\tilde{\nu}$ = 2954 s, 2922 s, 2851 s, 1568 vs, 1522 m, 1467 m, 1433 s, 1412 s, 1312 m, 740 m, 679 m cm^{-1}. − ^1H NMR ($CDCl_3$, room temp.): δ = 0.82 (t, 12 H, CH_3), 1.18 [m, 32 H, $CH_2(4-7)$], 1.54 [m, 8 H, $CH_2(3)$], 2.34 [t, 8 H, $CH_2(2)$]. − ^{13}C NMR ($CDCl_3$, room temp.): δ = 14.0 (CH_3), 22.6, 26.2, 29.1, 31.8, 37.5 (CH_2), 194.5 (CO_2).

$Mo_2(O_2C$-*n*$C_7H_{15})_4$: Prepared by a literature method.[9] − $C_{32}H_{60}Mo_2O_8$ (764.70): calcd. C 50.26, H 7.91; found C 50.77, H 8.10. − IR (KBr): $\tilde{\nu}$ = 2956 vs, 2929 vs, 2852 vs, 1506 vs, 1468 s, 1430 vs, 1412 vs, 1306 m, 1177 m, 1110 m, 802 m, 718 m, 657 m, 466 m cm^{-1}. − ^1H NMR ($CDCl_3$, room temp.): δ = 0.88 (t, 12 H, CH_3), 1.30 [m, 32 H, $CH_2(4-7)$], 1.80 [m, 8 H, $CH_2(3)$], 2.82 [t, 8 H, $CH_2(2)$]. − ^{13}C NMR ($CDCl_3$, room temp.): δ = 14.1 (CH_3), 22.7, 26.7, 29.1, 29.2, 31.9, 37.0 (CH_2), 185.7 (CO_2).

$Rh_2(O_2C$-*n*$C_7H_{15})_4(FPA)_2$ (1a): $Rh_2(O_2C$-*n*$C_7H_{15})_4$ (60 mg, 0.077 mmol) dissolved in 15 mL of CH_2Cl_2, was added to a 10 mL CH_2Cl_2 solution of FPA (49 mg, 0.17 mmol). After stirring at room temperature for 2 h, the solution was evaporated to dryness under vacuum and the residue was washed with *n*-hexane. The crude product obtained was purified by recrystallization from diethyl ether to give an orange powder. Yield: 90 mg, 86%. − $C_{66}H_{86}Fe_2N_2O_8Rh_2$ (1352.32): calcd. C 58.57, H 6.41, N 2.07; found C 58.22, H 6.80, N 2.03. − IR (KBr): $\tilde{\nu}$ = 2954 s, 2924 s, 2854 s, 2207 s, 1600 vs, 1587 vs, 1500 m, 1456 m, 1413 vs, 1314 m, 1214 m, 1170 m, 1107 m, 1011 m, 924 m, 826 m, 725 m, 677 m, 600 m, 540 m, 500 m, 486 m, 446 m cm^{-1}. − ^1H NMR ($CDCl_3$, room temp.): δ = 0.86 (t, 12 H, CH_3), 1.19 [m, 32 H, $CH_2(4-7)$], 1.42 [m, 8 H, $CH_2(3)$], 2.10 [t, 8 H, $CH_2(2)$], 4.29 (s, 10 H, C_5H_5), 4.33 [s, 4 H, $C_5H_4(\beta)$], 4.60 [s, 4 H, $C_5H_4(\alpha)$], 7.69 [s, br., 4 H, $C_5H_4N(\beta)$], 9.24 [s, br., 4 H, $C_5H_4N(\alpha)$]. − ^{13}C NMR ($CDCl_3$, room temp.): δ = 14.1 (CH_3), 22.6, 25.9, 28.9, 29.0, 31.7, 37.3 (CH_2), 63.5, 69.6, 70.2, 71.9 (C_5H_4 & C_5H_5), 83.8 [C≡*C*C_5H_4), 95.5 (NC_5H_4C≡C), 126.5 [$C_5H_4N(\beta)$], 133.1 [$C_5H_4N(\gamma)$], 150.8 [$C_5H_4N(\alpha)$], 194.2 (CO_2).

$Mo_2(O_2C$-*n*$C_7H_{15})_4$(FPA) (2a): A 20 mL diethyl ether solution containing $Mo_2(O_2C$-*n*$C_7H_{15})_4$ (122 mg,0.16 mmol) was added to a 20 mL diethyl ether solution of FPA (100 mg, 0.35 mmol). After stirring at room temperature for 2 h, the solution was evaporated to dryness under vacuum and the residue was washed with small portions of *n*-hexane. The orange product was obtained in a 65% yield (110 mg). − $C_{49}H_{73}FeMo_2NO_8Rh_2$ (1050.84): calcd. C 55.96, H 6.95, N 1.33; found C 55.32, H 7.10, N 1.28. − IR (KBr): $\tilde{\nu}$ = 2955 s, 2924 vs, 2853 s, 2202 s, 1601 s, 1507 vs, 1458 m, 1423 s, 1376 m, 1316 m, 1261 w, 1218 m, 1171 m, 1107 m, 1000 m, 928 m, 828 m, 801 m, 724 w, 645 w, 595 w, 542 w, 500 m, 446 w cm^{-1}. − ^1H NMR ($CDCl_3$, room temp.): δ = 0.88 (t, 12 H, CH_3), 1.29 [m, 32 H, $CH_2(4-7)$], 1.85 [m, 8 H, $CH_2(3)$], 2.92 [t, 8 H, $CH_2(2)$], 4.22 (s, 5 H, C_5H_5), 4.28 [s, 2 H, $C_5H_4(\beta)$], 4.50 [s, 2 H, $C_5H_4(\alpha)$], 7.22 [s, br., 2 H, $C_5H_4N(\beta)$], 8.30 [s, br., 2 H, $C_5H_4N(\alpha)$]. − ^{13}C NMR ($CDCl_3$, room temp.): δ = 14.1 (CH_3), 22.7, 26.7, 29.1, 29.2, 29.7, 31.8, 37.0 (CH_2), 63.4, 69.5, 70.1, 71.8 (C_5H_4 & C_5H_5), 83.3 (C≡*C*C_5H_4), 95.1 (NC_5H_4C≡C), 125.3 [$C_5H_4N(\beta)$], 132.9 [$C_5H_4N(\gamma)$], 149.4 [$C_5H_4N(\alpha)$], 185.4 (CO_2).

$Rh_2(O_2C$-*n*$C_7H_{15})_4(FP)_2$ (3a): $Rh_2(O_2C$-*n*$C_7H_{15})_4$ (100 mg, 0.13 mmol) and FP (74 mg, 0.28 mmol) were dissolved in 15 mL CH_2Cl_2. The solution was stirred at room temperature for 2 h, and evaporated to dryness under vacuum. The residue was washed with *n*-hexane and recrystallized in CH_2Cl_2/*n*-hexane. The orange product was obtained in a 71% yield (120 mg). − $C_{62}H_{86}Fe_2N_2O_8Rh_2$ (1304.88): calcd. C 57.07, H 6.64, N 2.15; found C 56.83, H 6.68, N 2.06. − IR (KBr): $\tilde{\nu}$ = 2954 m, 2924 s, 2854 m, 1605 s, 1585 vs, 1516 s, 1412 s, 1216 m, 1107 m,1034 w, 1017 m, 828 m, 687 m, 530 w, 498 m cm^{-1}. − ^1H NMR ($CDCl_3$, room temp.): δ = 0.86 (t, 12 H, CH_3), 1.20 [m, 32 H, $CH_2(4-7)$], 1.45 [m, 8 H, $CH_2(3)$], 2.12 [t, 8 H, $CH_2(2)$], 4.14 (s, 10 H, C_5H_5), 4.50 [t, 4 H, $C_5H_4(\beta)$], 4.86 [t, 4 H, $C_5H_4(\alpha)$], 7.67 [d, 4 H, $C_5H_4N(\beta)$], 9.93 [d, 4 H, $C_5H_4N(\alpha)$]. − ^{13}C NMR ($CDCl_3$, room temp.): δ = 14.1 (CH_3), 22.7, 25.9, 29.0, 29.1, 31.8, 37.3 (CH_2), 67.1, 70.1, 70.4, 81.0 (C_5H_4 & C_5H_5), 121.6, 149.8, 150.7 (C_5H_4N), 194.2 (CO_2).

$Rh_2(O_2CCH_3)_4(FP)_2$ (3b): A THF solution (20 mL) containing $Rh_2(O_2CCH_3)_4$ (57 mg, 0.13 mmol) and FP (75 mg, 0.28 mmol) was stirred at room temperature for 2 h, which led to an orange precipitate. The solvent was reduced to ca. 5 mL in vacuum, to which 20 mL of diethyl ether was added. The precipitate was collected and washed with 3 × 20 mL of diethyl ether. The orange product was purified by recrystallization in CH_2Cl_2/Et_2O. Yield: 110 mg (87%). − $C_{38}H_{38}Fe_2N_2O_8Rh_2$ (968.23): calcd. C 47.17, H 3.96, N 2.89; found C 47.63, H 4.17, N 2.63. − IR (KBr): $\tilde{\nu}$ = 3093 w, 2931 w, 1605 vs, 1590 vs, 1518 m, 1429 vs, 1343 m, 1290 w, 1223 m, 1108 m, 1016 m, 890 w, 836 m, 820 m, 694 m, 644 w, 627 w, 529 m, 518 m, 500 m, 434 w cm^{-1}. − ^1H NMR ($CDCl_3$, room temp.): δ = 1.93 (s, 12 H, CH_3), 4.14 (s, 10 H, C_5H_5), 4.51 [t, 4 H, $C_5H_4(\beta)$], 4.87 [t, 4 H, $C_5H_4(\alpha)$], 7.70 [d, 4 H, $C_5H_4N(\beta)$], 9.21 [d, 4 H, $C_5H_4N(\alpha)$]. − ^{13}C NMR ($CDCl_3$, room temp.): δ = 23.9 (CH_3), 67.2, 70.1, 70.5, 80.7 (C_5H_4 & C_5H_5), 121.7, 150.2, 150.6 (C_5H_4N), 191.9 (CO_2).

$Mo_2(O_2C$-*n*$C_7H_{15})_4(FP)_2$ (4a): $Mo_2(O_2C$-*n*$C_7H_{15})_4$ (100 mg, 0.13 mmol) and FP (69 mg, 0.26 mmol) were dissolved in 15 mL of CH_2Cl_2. The solution was stirred at room temperature for 2 h, and evaporated to dryness under vacuum. The residue was washed with *n*-hexane and recrystallized in CH_2Cl_2/*n*-hexane. The orange product was produced in a 53% yield (90 mg). − $C_{62}H_{86}Fe_2N_2O_8Mo_2$ (1304.88): calcd. C 57.07, H 6.64, N 2.15; found C 56.83, H 6.68, N 2.06. − IR (KBr): $\tilde{\nu}$ = 2955 s, 2919 s, 2852 s, 1506 vs, 1468 m, 1431 s, 1412 vs, 1315 w, 1109 m, 1031 w, 828 m, 718 m, 658 m, 466 m cm^{-1}. − ^1H NMR ($CDCl_3$, room temp.): δ = 0.88 (t, 12 H, CH_3), 1.30−1.41 [m, 32 H, $CH_2(4-7)$], 1.87 [m, 8 H, $CH_2(3)$], 2.96 [t, 8 H, $CH_2(2)$], 4.00 (s, 10 H, C_5H_5), 4.40 [t, 4 H, $C_5H_4(\beta)$], 4.66

[t, 4 H, C_5H_4(α)], 7.21 [d, 4 H, C_5H_4N(β)], 8.21 [d, 4 H, C_5H_4N(α)]. − ^{13}C NMR ($CDCl_3$, room temp.): δ = 14.1 (CH_3), 22.7, 26.7, 29.0, 29.1, 29.2, 31.8, 37.1 (CH_2), 66.9, 70.0, 70.3, 80.6 (C_5H_4 & C_5H_5), 120.5, 149.6 (C_5H_4N), 185.4 (CO_2).

$Mo_2(O_2CCF_3)_4(FP)_2$ (4b): $Mo_2(O_2CCF_3)_4$ (102 mg, 0.16 mmol) and FP (91 mg, 0.35 mmol) were dissolved in 15 mL of CH_2Cl_2. The solution was stirred at room temperature for 2 h, and evaporated to dryness under vacuum. The residue was washed with *n*-hexane and recrystallized in CH_2Cl_2/*n*-hexane. The orange product was obtained in a 96% yield (180 mg). − $C_{38}H_{26}F_{12}Fe_2Mo_2N_2O_8$ (1170.19): calcd. C 39.00, H 2.24, N 2.39; found C 39.20, H 2.52, N 2.51. − IR (KBr): $\tilde{\nu}$ = 1684 m, 1631m, 1603 vs, 1520 m, 1428 m, 1194 vs, 1160 s, 1108 w, 1031 w, 1014 m, 1003 m, 856 m, 822 m, 778 w, 730 s, 684 m, 527 m, 496 m cm^{-1}. − ^{1}H NMR ($CDCl_3$, room temp.): δ = 3.99 (s, 10 H, C_5H_5), 4.42 [t, 4 H, C_5H_4(β)], 4.64 [t, 4 H, C_5H_4(α)], 7.19 [d, 4 H, C_5H_4N(β)], 7.90 [d, 4 H, C_5H_4N(α)]. − ^{13}C NMR ($CDCl_3$, room temp.): δ = 67.0, 70.1, 70.7, 79.8 (C_5H_4 & C_5H_5), 114.9 (CF_3), 124.2, 148.7, 151.1 (C_5H_4N), 166.1 (CO_2). − ^{19}F NMR ($CDCl_3$, room temp.): δ = −9.29.

$[Rh_2(O_2C\text{-}nC_7H_{15})_4(BPEF)]_n$ (5): A mixture of $Rh_2(O_2C\text{-}nC_7H_{15})_4$ (117 mg, 0.15 mmol) and BPEF (58 mg, 0.15 mmol) was dissolved in 25 mL of dichloromethane. The solution was stirred at room temperature overnight, and then filtered to remove traces of the precipitate. The filtrate was then evaporated to dryness under vacuum. The crude product was washed with diethyl ether and recrystallized by diffusion of diethyl ether into its dichloromethane solution. The deep orange product was obtained in a 86% yield (150 mg). − $[C_{56}H_{76}FeN_2O_8Rh_2]_n$ ($n \times$ 1166.31): calcd. C 57.62, H 6.57, N 2.40; found C 57.38, H 6.30, N 2.43. − IR (KBr): $\tilde{\nu}$ = 2955 s, 2925 s, 2853 s, 2211 s, 1600 s, 1588 vs, 1500 m, 1458 m, 1413 s, 1314 m, 1215 m, 1172 w, 1010 m, 925 w, 826 m, 730 w, 669 w, 601 w, 550 w, 496 m cm^{-1}. − ^{1}H NMR ($CDCl_3$, room temp.): δ = 0.85 (t, 12 H, CH_3), 1.19 [m, 32 H, CH_2(4−7)], 1.43 [m, 8 H, CH_2(3)], 2.11 [t, 8 H, CH_2(2)], 4.50 [s, 4 H, C_5H_4(β)], 4.71 [s, 4 H, C_5H_4(α)], 7.72 [d, 4 H, C_5H_4N(β)], 9.26 [d, 4 H, C_5H_4N(α)]. − ^{13}C NMR ($CDCl_3$, room temp.): δ = 14.1 (CH_3), 22.6, 25.9, 29.0, 31.7, 37.3 (CH_2), 65.1, 72.5, 73.5 (C_5H_4), 84.5 (C≡*C*C_5H_4), 94.3 (NC_5H_4*C*≡C), 126.5 [C_5H_4N(β)], 132.8 [C_5H_4N(γ)], 150.9 [C_5H_4N(α)], 194.2 (CO_2).

$[Mo_2(O_2C\text{-}nC_7H_{15})_4]_2(BPEF)$ (6): A mixture of $Mo_2(O_2C\text{-}nC_7H_{15})_4$ (128 mg, 0.17 mmol) and BPEF (65 mg, 0.17 mmol) was dissolved in 20 mL of dichloromethane. The solution was stirred at room temperature overnight, and the solvent was then evaporated to dryness under vacuum. The residue was washed with one portion of 5 mL of diethyl ether and several portions of *n*-hexane. The pale-orange powder was recrystallized from CH_2Cl_2/*n*-hexane. Yield: 80 mg, 49% yield based on $Mo_2(O_2C\text{-}nC_7H_{15})_4$. − $C_{88}H_{136}FeMo_4N_2O_{16}$ (1917.66): calcd. C 55.12, H 7.15, N 1.46; found C 54.78, H 6.80, N 1.60. − IR (KBr): $\tilde{\nu}$ = 2956 vs, 2920 vs, 2852 vs, 2207 m, 1596 m, 1506 vs, 1458 m, 1430 s, 1412 vs, 1315 m, 1257 w, 1213 w, 1177 m, 1110 m, 1026 w, 928 w, 874 w, 816 m, 718 m, 657 m, 541 w, 489 m, 466 m, 444 m cm^{-1}. − ^{1}H NMR ($CDCl_3$, room temp.): δ = 0.88 (t, 24 H, CH_3), 1.29 [m, 64 H, CH_2(4−7)], 1.83 [m, 16 H, CH_2(3)], 2.90 [t, 16 H, CH_2(2)], 4.35 [t, 4 H, C_5H_4(β)], 4.54 [t, 4 H, C_5H_4(α)], 7.15 [d, 4 H, C_5H_4N(β)], 8.31 [d, 4 H, C_5H_4N(α)]. − ^{13}C NMR ($CDCl_3$, room temp.): δ = 14.1 (CH_3), 22.7, 26.7, 29.1, 29.2, 31.8, 37.0 (CH_2), 65.4, 71.8, 73.4 (C_5H_4), 84.2 (C≡*C*C_5H_4), 125.2 [C_5H_4N(β)], 132.6 [C_5H_4N(γ)], 149.4 [C_5H_4N(α)], 185.6 (CO_2).

Acknowledgments

W. M. X. thanks the Bayerische Forschungsstiftung for a postdoctoral research associate fellowship. Professor W. A. Herrmann is acknowledged for the continuous support of our work. The authors are also grateful to the Fonds der Chemischen Industrie for financial support. Dr. É. S. Bencze is acknowledged for recording the vibrational spectra.

[1] F. A. Cotton, R. A. Walton, *Multiple Bonds between Metal Atoms*, 2nd edn., Oxford University Press, London, **1993** and references therein.

[2] [2a] M. H. Chisholm, *Acc. Chem. Res.* **2000**, *33*, 53−61. − [2b] R. H. Cayton, M. H. Chisholm, J. C. Huffman, E. B. Lobkovsky, *J. Am. Chem. Soc.* **1991**, *113*, 8709−8724. − [2c] F. A. Cotton, C. Lin, C. A. Murillo, *J. Chem. Soc., Dalton Trans.* **1998**, 3151−3153.

[3] [3a] F. A. Cotton, J. G. Norman, *J. Coord. Chem.* **1971**, *1*, 161. − [3b] B. Morosin, R. C. Hughes, Z. G. Soos, *Acta Crystallogr.* **1975**, *B31*, 762−770. − [3c] F. A. Cotton, T. R. Felthouse, *Inorg. Chem.* **1980**, *19*, 328−331. − [3d] F. A. Cotton, T. R. Felthouse, *Inorg. Chem.* **1981**, *20*, 600−608. − [3e] M. Handa, K. Kasamatsu, K. Kasuge, M. Mikuriya, T. Fujii, *Chem. Lett.* **1990**, 1753−1756. − [3f] M. C. Kerby, B. W. Eichhorn, J. A. Creighton, K. P. C. Vollhardt, *Inorg. Chem.* **1990**, *29*, 1319−1323. − [3g] F. A. Cotton, Y. Kim, T. Ren, *Inorg. Chem.* **1992**, *31*, 2723−2726. − [3h] X. Ouyang, C. Campana, K. R. Dunbar, *Inorg. Chem.* **1996**, *35*, 7188−7189. − [3i] J. L. Wesemann, M. H. Chisholm, *Inorg. Chem*. **1997**, *36*, 3258−3267. − [3j] M. Handa, H. Matsumoto, D. Yashioka, R. Nukada, M. Mikuriya, I. Hiromitsu, K. Kasuge, *Bull. Chem. Soc. Jpn.* **1998**, *71*, 1811−1816. − [3k] M. Handa, M. Watanabe, D. Yashioka, S. Kawabata, R. Nukada, M. Mikuriya, H. Azuma, K. Kasuge, *Bull. Chem. Soc. Jpn.* **1999**, *72*, 2681−2686. − [3l] Y. Ding, S. S. Lau, P. E. Fanwick, R. A. Walton, *Inorg. Chim. Acta* **2000**, *300−302*, 505−511. − [3m] T. Ren, G. Zou, J. C. Alvarez, *Chem. Commun.* **2000**, 1197−1198. − [3n] K.-T. Wong, J.-M. Lehn, S.-M. Peng, G.-H. Lee, *Chem. Commun.* **2000**, 2259−2260.

[4] [4a] W.-M. Xue, F. E. Kühn, E. Herdtweck, Q. Li, *Eur. J. Inorg. Chem.* **2001**, 213−221. − [4b] A. M. Santos, F. E. Kühn, W.-M. Xue, E. Herdtweck, *J. Chem. Soc., Dalton Trans.* **2000**, 3570−3574.

[5] [5a] W.-M. Xue, F. E. Kühn, G. Zhang, E. Herdtweck, *J. Organomet. Chem.* **2000**, *596*, 177−182. − [5b] W.-M. Xue, F. E. Kühn, G. Zhang, E. Herdtweck, G. Raudaschl-Sieber, *J. Chem. Soc., Dalton Trans.* **1999**, 4103−4110.

[6] T. H. Barr, W. E. Watts, *J. Organomet. Chem.* **1968**, *15*, 177−185.

[7] T. M. Miller, K. J. Ahmed, M. S. Wrighton, *Inorg. Chem.* **1989**, *28*, 2347−2355.

[8] A.-M. Girond-Godquin, J.-C. Marchon, *J. Phys. Chem.* **1986**, *90*, 5502−5503.

[9] R. H. Cayton, M. H. Chisholm, F. D. Darrington, *Angew. Chem. Int. Ed. Engl.* **1990**, *29*, 1481−1483.

Received November 30, 2000
[I00457]